

Measurement of Impulse Response of Shallow Water Communication Channel by Correlation Method

Jan SCHMIDT, Iwona KOCHAŃSKA, Aleksander SCHMIDT

Gdansk University of Technology,
Faculty of Electronics, Telecommunication and Informatics,
Department of Marine Electronics Systems
G. Narutowicza 11/12, 80-233 Gdansk, Poland
jan.schmidt@pg.edu.pl

Performances of underwater acoustic communication (UAC) systems are strongly related to specific propagation conditions of the underwater channel; conditions that can additionally change in time due to the movement of the acoustic system transmitter and receiver or to reflection by underwater objects of the transmitted signal. The time-varying impulse response is a comprehensive description of dynamically changing transmission properties of the UAC channel. It is a basis for estimation of stochastic parameters used for designing the signaling scheme of the communication system. The paper presents the results of a measurement experiment conducted in a shallow water environment. The channel impulse response was measured by the correlation method with the use of two kinds of broadband signals: pseudo-random binary sequence (PRBS) and hyperbolic frequency modulation chirp (HFM). For each measurement result statistical transmission parameters, namely delay spread, Doppler spread, coherence time, and coherence bandwidth were estimated.

Keywords: underwater communications, impulse response, delay spread, Doppler spread, coherence time, coherence bandwidth, PRBS, HFM

1. Introduction

Propagation conditions of the underwater acoustic communication (UAC) channel depend on its geometry, geographic location, and they additionally change over time. Thus, there is a diversity of underwater acoustic channels between the transmitter and receiver of communication system. Time-varying channel impulse response measurement is necessary to model the UAC channel and simulate communication system performance [5]. Moreover, the channel impulse response is the basis for estimation of a set of statistical parameters, namely delay spread, Doppler spread, coherence time and coherence bandwidth, that are used to

design the physical layer of data transmission: as much resistant as possible to distortions caused by the time-varying multipath propagation conditions [1].

Numerous underwater impulse response estimates were gathered during the shallow-water measurement experiment by the correlation method. Two types of probe signals were used: PRBSs. and HFM chirp trains. The results of the measurements are the basis for statistical analysis of transmission properties of the measured communication channel.

2. Correlation Method of Impulse Response Measurement

Underwater acoustic communication channel can be characterized by a time-variant impulse response $h(t, \tau)$ defined in a window of observation time t and delay τ . In the case of a bandlimited bandpass channel the impulse response can be equivalently described by a complex baseband impulse response $h_b(t, \tau)$, further referred to as a channel impulse response (CIR), with the input and output being the complex envelope of transmitted and received signal, respectively [2]:

$$r_b(t) = \frac{1}{2} s_b(t) * h_b(t, \tau) \quad (1)$$

where $s_b(t)$ and $r_b(t)$ are the complex envelopes of transmitted $s(t)$ and received signal $r(t)$:

$$s(t) = \text{Re}\{s_b(t) \exp(j2\pi f_c t)\} \quad (2)$$

$$r(t) = \text{Re}\{r_b(t) \exp(j2\pi f_c t)\} \quad (3)$$

The channel impulse response measurement was performed by the correlation method. Two types of probe signals were used, namely pseudorandom binary sequences (PRBSs) and hyperbolic frequency-modulated (HFM) chirp trains. Both types of signals have a narrow, impulse-like autocorrelation function, as is shown in Fig.2.

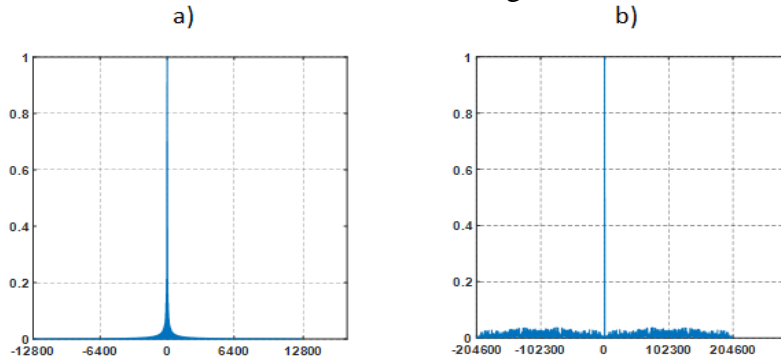


Fig. 1. Autocorrelation function of HFM (a) and PRBS (b) training signals.

A single hyperbolic frequency modulation chirp with increasing frequency is described with the equation:

$$s_{HFM\uparrow}(t) = \exp\left(-j2\pi \frac{\ln\left(kt + \frac{1}{f_1}\right)}{k}\right) \quad (4)$$

where $k = (f_1 - f_2)/(f_1 f_2 T_s)$, with f_1 and f_2 being minimal and maximal frequency, respectively, and T_s being a single chirp duration. A structure of probe signal, based on $s_{HFM\uparrow}(t)$ is shown in Fig.3. Every two subsequent chirps are separated with a guard interval of duration T_g .

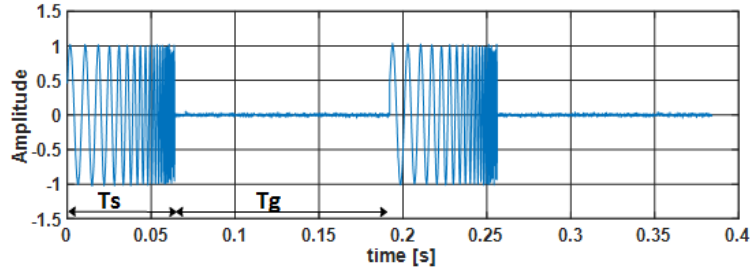


Fig. 2. Structure of HFM-based probe signal

The PRBS train is a repetition of a maximal-length bit sequence $c_m \in \{-1; 1\}$, modulated onto a binary phase-shift keyed waveform:

$$s_{PRBS}(t) = \sin(2\pi f_c t) \sum_{m=0}^{M-1} c_m \text{rect}\left(t - \frac{m}{M}T\right) \quad (5)$$

where $T = f_s/\Delta B$, f_s is sampling frequency, ΔB is signal bandwidth, f_c is carrier frequency, and the sequence length $M = 2^L - 1$ is determined by its order L . The probe signal $s(t)$ is constructed of K subsequent s_{PRBS} of duration T_s , without any pause in between.

At the receiver, the analog signal $r(t)$ from the ultrasonic transducer is digitized by an analog-to-digital converter. Then, digital samples are passed to a digital down converter (DDC) to translate a real-value pass-band signal $r[n]$ centered around the selected carrier frequency down to a complex base-band signal $r_b[n]$, centered around zero frequency [3]. It removes all undesirable signals by low-pass filtering, and reduces the sampling rate. An estimate of discrete channel impulse response $\hat{h}_b[n]$ is obtained as the cross-correlation function of $r_b[n]$ and $s_b[n]$, that is an analytic signal with its real part equal to probe signal $s[n]$ and imaginary part equal to Hilbert transform of $s[n]$:

$$\hat{h}_b[n] = (r_b * s_b)[n] = (s_b * h_b * s_b)[n] = (h_b * R_s)[n] \quad (6)$$

where $0 \leq n < K$, K is the number of samples, and $R_s[n]$ is an autocorrelation function of probe signal $s_b[n]$. Subsequent estimates obtained due to measuring the channel with the same repeated probe signal constitute the two-dimensional complex value estimate of time-varying impulse response $h_b(t, \tau)$.

3. Experiment

Channel measurements were conducted on the 4th and 5th of May this year, in Wdzydze Lake. Figure 3 shows the configuration of experiment. Each signal probe was generated using the MATLAB platform. Conversion to analogue signal was performed using digital-to-analogue converter from an NI USB-6363 device. Next, signal was amplified and transmitted to water by underwater telephone HTL-10 [3]. This transmission stand was placed on board the boat. The same equipment was used in the receiving stand, but otherwise was configured. The receiving equipment was placed in the measuring container whose position was fixed. Transmission transducer was dipped to a depth h_{Tx} of 10 meters, regardless of water depth of about 20-30 meters. Receiving transducer was dipped to a depth h_{Rx} of 4 meters, at a constant depth of water of 7 meters. The distances between transmission and receiving stand were 340, 550 and 1035 meters.

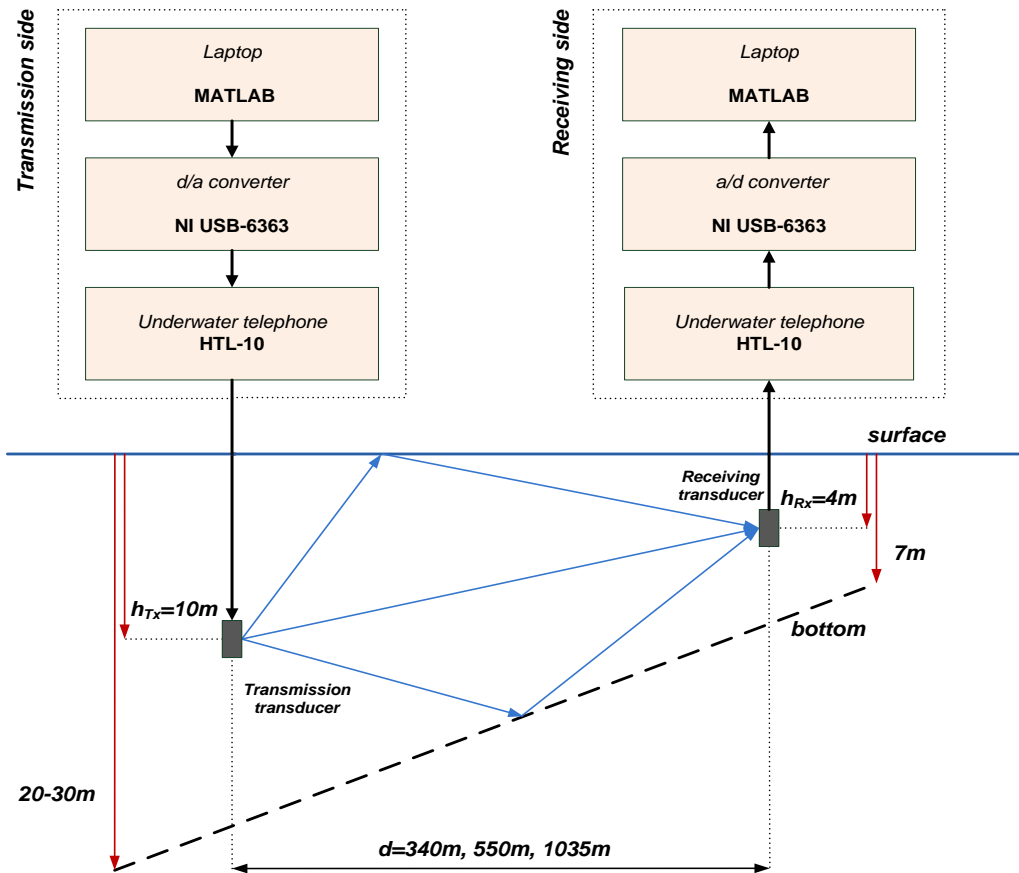


Fig.3 Measuring system

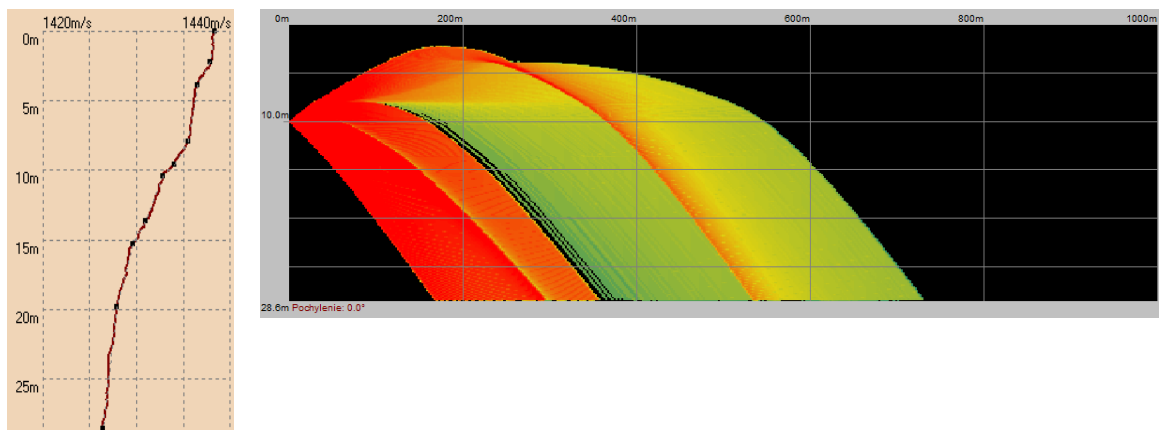


Fig.4 Measured sound speed profile and estimated range

Prior to the measurement series, a sound speed profile was determined using sound speed meter depending on the depth. Measured profile and based on this, the range of the communication system was estimated by defining sound propagation paths, as shown in Figure 4. This sound speed profile guarantees favorable propagation conditions.

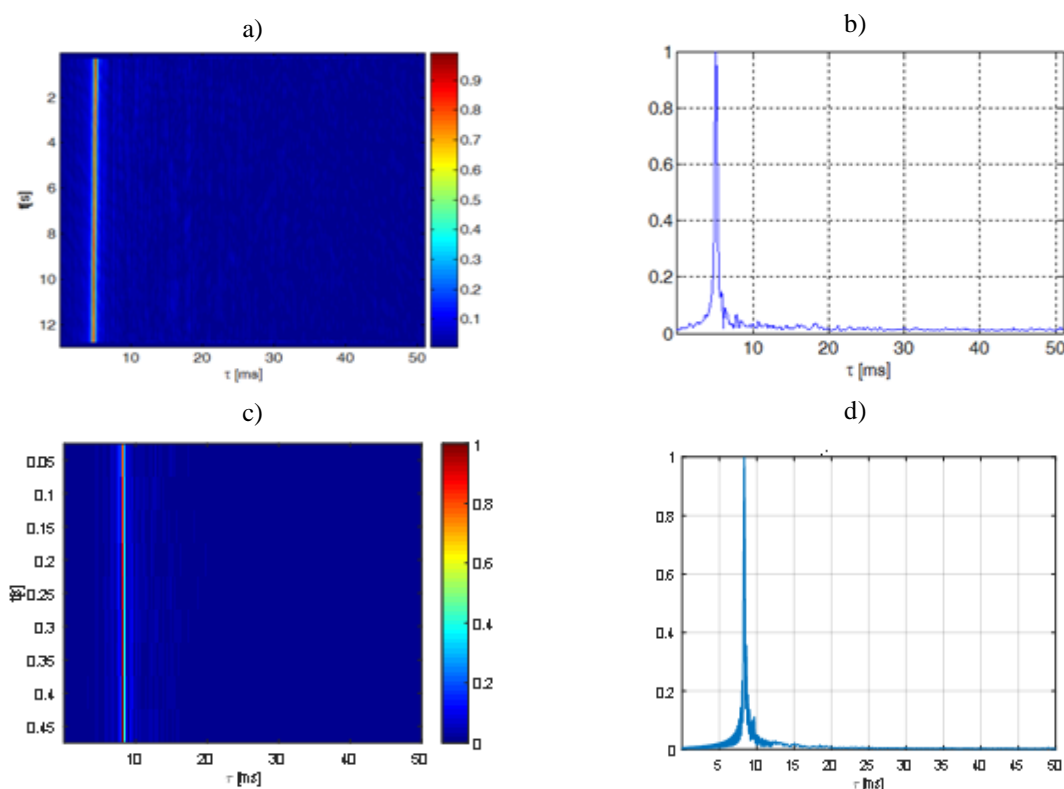


Fig. 5. Results of measurement at a distance of 340 m in bandwidth of 5kHz: module of CIR measured with PRBS (a) and its average over t-axis (b); module of CIR measured with HFM (c) and its average over t-axis (d).

A single PRBS probe signal was based on an m-sequence of rank 8, and its duration was $T_s = 25.5ms$ or $T_s = 51ms$. It was repeated up to 127 times to gather one time-varying channel impulse response. A single HFM probe signal consisted of a chirp of duration $T_s = 64ms$ and a guard interval $T_g = 128ms$. Carrier frequency of these two signal types has been set to $f_c = 30kHz$. It was repeated no more than 20 times during one measurement. The channel was measured by signals occupying two bandwidths: $B = 5kHz$ and $B = 10kHz$. For both cases a sampling frequency was equal to $f_s = 200kHz$.

The modules of complex value channel impulse responses obtained at the three different distances, with the use of two kinds of probe signals of bandwidth $B = 5kHz$ are shown in Fig. 5-7. The general character of the presented impulse responses can be regarded as convergent, while the differences occur due to the peculiar characteristics of the individual signal to be transmitted over the channel. PRBS probe signals were shorter, than HFM signals, and there were a long guard time in the latter case. On the other hand, there was significantly less repetitions of HFM probe signals than PRBS sequences, that is clearly seen as lower resolution of channel impulse responses (along the t-axis) obtained by the first kind of signal.

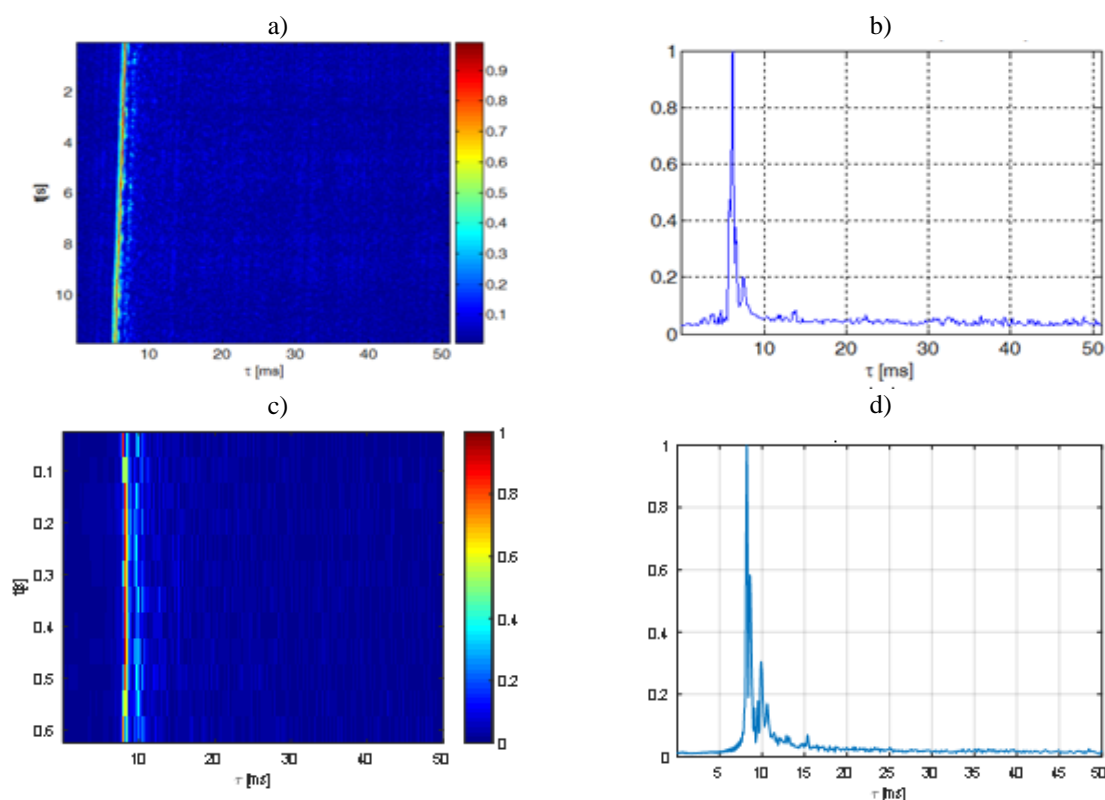


Fig. 6. Results of measurement at a distance of 550 m in bandwidth of 5kHz: module of CIR measured with PRBS (a) and its average over t-axis (b); module of CIR measured with HFM (c) and its average over t-axis (d).

4. Transmission Characteristics of UAC channel

The channel impulse response $h_b(t, \tau)$ is the basis for calculating numerous transmission characteristics, describing time and frequency dispersion and variability, as it shown in Fig. 8. The power delay profile $P_\tau(\tau)$ is calculated as an average of $|h_b(t, \tau)|^2$ over the t variable. There are several metrics of time dispersion of the channel, which are calculated on the basis of $P_\tau(\tau)$. One of them is the excess delay spread $\tau_{\rho dB}$, which is calculated as the delay between the first and last multipath component of $P_\tau(\tau)$ at a given threshold ρ [dB]. Other parameters are: mean delay spread τ_m and rms delay spread τ_{rms} [4]:

$$\tau_m = \frac{\sum_k P_\tau(\tau_k) \tau_k}{\sum_k P_\tau(\tau_k)} \quad (7)$$

$$\tau_{rms} = \sqrt{\overline{\tau^2} - \tau_m^2} \quad (8)$$

where

$$\overline{\tau^2} = \frac{\sum_k P_\tau(\tau_k) \tau_k^2}{\sum_k P_\tau(\tau_k)} \quad (9)$$

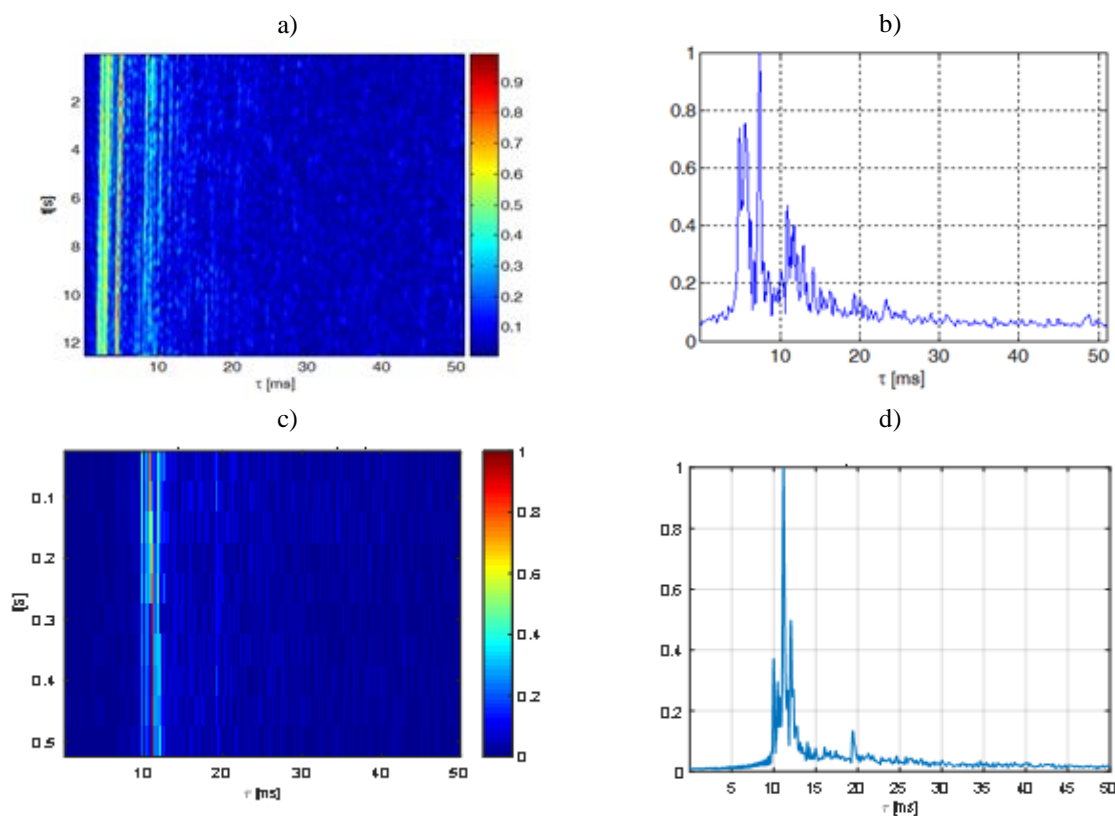


Fig. 7. Results of measurement at a distance of 1035 m in bandwidth of 5kHz: module of CIR measured with PRBS (a) and its average over t -axis (b); module of CIR measured with HFM (c) and its average over t -axis (d).

Time-varying transfer function $H(t, f)$ of the channel is calculated as the Fourier transform of $h_b(t, \tau)$. To characterize the frequency selectivity of the channel, the autocorrelation function of $H(t, f)$ is calculated:

$$R_H(t, \Delta f) = E\{H(t, f)H^*(t, f + \Delta f)\} \quad (10)$$

The frequency-correlation function $R_H(f)$ is obtained as the average of $R_H(t, \Delta f)$, and the coherence bandwidth B_C is calculated as the width of $R_H(f)$ at a given threshold ρ . The time-variance of the channel can be characterized in observation time domain t or Doppler shift domain ν . In both cases the autocorrelation function of $h_b(t, \tau)$ is a basis for further analysis:

$$R_h(\Delta t, \tau) = E\{h_b(t, \tau)h_b^*(t + \Delta t, \tau)\} \quad (11)$$

The width at a given threshold of averaged time-correlation function $R_h(\Delta t, \tau)$ is used to define coherence time T_C as a time interval, at which CIR remains constant.

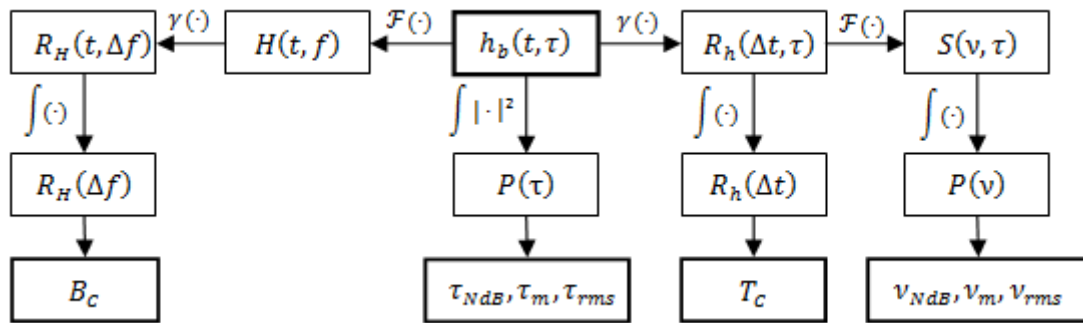


Fig. 8. Transmission characteristics of wireless channel; $\mathcal{F}(\cdot)$ - Fourier transform, $\gamma(\cdot)$ - autocorrelation function.

The scattering function $S_h(\nu, \tau)$ of the channel is obtained as the Fourier transform of $R_h(\Delta t, \tau)$. The Doppler power spectral density $P_\nu(\nu)$ is an average of $S_h(\nu, \tau)$ over delay domain τ . The Doppler spread of transmitted signal, being a consequence of time-variance of the channel, can be described similarly as the delay spread in the time domain, that is as a maximum Doppler shift $\nu_{\rho dB}$ at a given threshold ρ (calculated as the width of $P_\nu(\nu)$), mean Doppler spread ν_m , and rms Doppler spread ν_{rms} [4]:

$$\nu_m = \frac{\sum_k P_\nu(\nu_k) \nu_k}{\sum_k P_\nu(\nu_k)} \tag{12}$$

$$\nu_{rms} = \sqrt{\overline{\nu^2} - \nu_m^2} \tag{13}$$

where

$$\overline{\nu^2} = \frac{\sum_k P_\nu(\nu_k) \nu_k^2}{\sum_k P_\nu(\nu_k)} \tag{14}$$

The structure of the probe signal has a direct impact on the resolution of measured impulse response, and thus on the estimated transmission parameters. The resolution of time- and frequency domain variables of channel characteristics estimated for CIR measured with different probe signals, repeated K times, are shown in Table 1.

Tab.1. Resolution of channel transmission characteristics estimated for CIR measured with different probe signals.

B	signal	T_s	T_g	K	r_τ	r_t	r_f	r_ν
5 kHz	HFM	64.0 ms	128 ms	20	0.2 ms	192 ms	15.62 Hz	0.26 Hz
5 kHz	PRBS	51.0 ms	0	127	0.2 ms	51.0 ms	19.61 Hz	0.15 Hz
10 kHz	HFM	64.0 ms	128 ms	20	0.1 ms	192 ms	15.62 Hz	0.26 Hz
10 kHz	PRBS	25.5 ms	0	127	0.1 ms	25.5 ms	39.21 Hz	0.31 Hz

The resolution of time delay r_τ is equal to the reciprocal of probe signal bandwidth B ($r_\tau = 1/B$). The resolution of observation time r_t depends on the probe signal duration T_s including guard time T_g ($r_t = T_s + T_g$). In the frequency domain the transfer function of the channel can be calculated with the frequency step equal to the reciprocal of probe signal

duration T_s ($r_f = 1/T_s$). Finally, Doppler power spectrum density can be analyzed with Doppler shift resolution dependent on the probe signal duration T_s , guard time T_g and number of probe signal repetitions K : $r_v = 1/K(T_s + T_g)$. Table 1 presents the resolution values for HFM and PRBS signals used during the measurement experiment.

Table 2 presents the results of estimation of the transmission parameters. Significant differences of obtained values due to the type of probe signal are clearly seen. The smallest differences were observed for excess delay spread τ_{10dB} and maximum Doppler spread ν_{10dB} , as well as coherence bandwidth $B_{c0.9}$ and coherence time $T_{c0.9}$ measured as the width of appropriate correlation function on the level of 0.9 of maximum value.

Tab.2. Transmission parameters estimated on the basis of CIR measured with different probe signals

d [m]	B [kHz]	signal	τ_{10dB} [ms]	τ_m [ms]	τ_{rms} [ms]	$T_{c0.5}$ [s]	$T_{c0.9}$ [s]	$B_{c0.5}$ [Hz]	$B_{c0.9}$ [Hz]	ν_{10dB} [ms]	ν_m [ms]	ν_{rms} [ms]
340	5.0	HFM	0.35	8.17	1.58	0.90	0.20	4120	1000	1.21	0	1.32
340	5.0	PRBS	0.57	5.84	4.69	8.77	1.22	1921	313.7	1.59	0.79	0.42
340	10	HFM	0.15	8.23	1.37	0.80	0.20	9280	1800	1.29	0	1.36
340	10	PRBS	0.32	5.34	2.23	4.90	0.97	2745	470.6	1.65	0.79	0.58
550	5.0	HFM	0.69	9.82	6.08	0.60	0.10	1140	80.00	1.74	0	2.00
550	5.0	PRBS	0.97	10.29	9.97	0.41	0.10	549.0	39.22	6.98	3.18	2.06
550	10	HFM	1.95	9.40	4.14	4.00	0.40	600.0	120.0	0.19	0	1.42
550	10	PRBS	1.86	7.48	4.01	0.26	0.10	549.0	78.43	4.53	1.17	2.39
1035	5.0	HFM	4.03	10.4	10.97	0.70	0.20	280.0	40.00	1.03	0	1.98
1035	5.0	PRBS	8.36	11.0	9.22	4.49	0.31	117.6	39.22	2.73	1.25	0.84
1035	10	HFM	2.41	6.58	6.29	0.60	0.20	680.0	120.0	1.60	0	1.79
1035	10	PRBS	7.71	9.38	4.43	2.09	0.31	156.8	78.43	2.12	0.96	1.25

5. Conclusions

The underwater channel impulse responses of shallow inland water were measured by the correlation method during the experiment performed in Wdzydze Lake. Two kinds of probe signals were used: HFM and PRBS, both having a narrow, impulse-like autocorrelation function. As a result of the analysis of measured CIRs transmission parameters were estimated, describing time and frequency dispersion and variability of the UAC channel. Significant differences in parameters values were observed due to the type and bandwidth of probe signal used. In the case of delay spread and Doppler spread, the values measured at the threshold of 10dB seem to be potentially useful for designing the physical layer of data transmission, as the results of τ_{10dB} and ν_{10dB} are most convergent regardless of the type of probe signal. The use of mean and rms parameters requires further research to clarify the effect of the measurement signal on their values. It is also necessary to perform analysis of the influence of the bandwidth of measurement signal on CIRs and transmission parameters, especially on the coherence bandwidth value.

References

- [1] I. Kochanska, J. Schmidt, and M. Rudnicki, Underwater Acoustic Communications in Time-Varying Dispersive Channels, Federated Conference on Computer Science and Information Systems, M. Ganzha, L. Maciaszek, M. Paprzycki (eds). ACSIS, vol. 8, pp. 467–474, 2016.
- [2] L. E. Franks, Carrier and Bit Synchronization in Data Communication – A Tutorial Review, IEEE Transactions on Communications, Vol. COM-28, No. 8, pp. 1107 – 1121, 1980.
- [3] J. Schmidt, The development of an underwater telephone for digital communication purposes, Hydroacoustics vol. 19 , pp. 341-352, 2016.
- [4] T. S. Rappaport, Wireless Communications: Principles and Practice, Second Edition, Prentice Hall, 2002.
- [5] R. Studanski, A. Zak, Measurement of Hydroacoustic Channel Impulse Response, Applied Mechanics and Materials, vol. 817, pp. 317-324, 2016.